

¹ **Magnitude-sensitive reaction times**

² **reveal non-linear time costs in**

³ **multi-alternative decision-making**

⁴ **James A. R. Marshall^{1*}, Andreagiovanni Reina^{1,2}, Célia Hay³, Audrey Dussutour³,**
⁵ **Angelo Pirrone⁴**

***For correspondence:**

james_marshall@sheffield.ac.uk
(JARM)

⁶ ¹Department of Computer Science, University of Sheffield, UK; ²IRIDIA, Université Libre
⁷ de Bruxelles, Belgium; ³Research Centre for Animal Cognition (CRCA), Centre for
⁸ Integrative Biology (CBI), Toulouse University, France; ⁴Centre for Philosophy of Natural
⁹ and Social Science, London School of Economics and Political Science, UK

¹⁰ **Abstract**

¹¹ Optimality analysis of value-based decisions in binary and multi-alternative choice settings predicts
¹² that reaction times should be sensitive only to differences in stimulus magnitudes, but not to overall
¹³ absolute stimulus magnitude. Yet experimental work in the binary case has shown magnitude
¹⁴ sensitive reaction times, and theory shows that this can be explained by switching from linear
¹⁵ to geometric time costs, but also by nonlinear subjective utility. Thus disentangling explanations
¹⁶ for observed magnitude sensitive reaction times is difficult. Here for the first time we extend the
¹⁷ theoretical analysis of geometric time-discounting to ternary choices, and present novel experi-
¹⁸ mental evidence for magnitude-sensitivity in such decisions, in both humans and slime moulds.
¹⁹ We consider the optimal policies for all possible combinations of linear and geometric time costs,
²⁰ and linear and nonlinear utility; interestingly, geometric discounting emerges as the predominant
²¹ explanation for magnitude sensitivity.

²² **Introduction**

²³ While the normative, optimal policy, approach to understanding decision-making is now well
²⁴ established for perceptual decisions (e.g. *Bogacz et al. (2006)*), it has only recently been applied to
²⁵ value-based decisions (*Fudenberg et al., 2018; Tajima et al., 2016, 2019*); such decisions differ from
²⁶ perceptual decisions because decision makers are rewarded by the value of the selected option,
²⁷ rather than whether or not they selected the best option (e.g. *Pirrone et al. (2014); Tajima et al.*
²⁸ *(2016, 2019); Krajbich et al. (2010)*). Recently researchers have analysed multi-alternative value-
²⁹ based decision-making (*Tajima et al., 2019*), building on earlier work in optimal decision policies

30 for binary value-based choices (*Tajima et al., 2016*). Through sophisticated analysis based on the
31 standard tool for solving such decision problems, stochastic dynamic programming (*Mangel and*
32 *Clark, 1988; Houston and McNamara, 1999*), the authors also present neurally-plausible decision
33 mechanisms that may implement or approximate the optimal decision policies (*Tajima et al.,*
34 *2016, 2019*). These policies turn out to be described by rather simple and well-known decision
35 mechanisms, such as drift-diffusion models with decision thresholds that collapse over time for the
36 binary case (*Tajima et al., 2016*), and nonlinear time-varying thresholds that interpolate between
37 best-vs-average and best-vs-next in the multi-alternative case (*Tajima et al., 2019*).

38 Interestingly, the theoretically optimal policy for the binary decision case (*Tajima et al., 2016*) is
39 inconsistent with empirical observations of magnitude-sensitive reaction-times (*Teodorescu et al.*
40 *(2016); Pirrone et al. (2018a); Stevenson et al. (2019); Zajkowski et al. (2019); Turner et al. (2019)*,
41 but see *Bhui (2019)*), unless assumptions are made that subjective utilities for decision-makers
42 are nonlinear, or decisions are embedded in a fixed-length time period with known or learnable
43 distributions of trial option values, so that a variable opportunity cost arises from decision time
44 (*Tajima et al., 2016*). Furthermore, even single-trial dynamics lead to magnitude sensitive reaction
45 times (*Pirrone et al., 2018b*).

46 Previous analyses made an assumption that appears widespread in psychology and neuro-
47 science, that decision-makers should optimise their Bayes Risk from such decisions (*Tajima et al.*
48 *2016, 2019*); this is equivalent to maximising the expected value of decisions in which there is a
49 linear cost for the time spent deciding (*Bogacz et al., 2006; Pirrone et al., 2014*). For a lab subject in
50 a pre-defined and known experimental design this may appear appropriate, for example because
51 there may be a fixed time duration within which a number of decision trials will occur and the
52 subject can learn the value distribution of the trials (e.g. *Bogacz et al. (2006); Pirrone et al. (2014)*).
53 However, an alternative and standard formulation of the Bellman equation, the central equation
54 in constructing a dynamic program, accounts for the cost of time by discounting future rewards
55 geometrically, so a reward one time step in the future is discounted by rate $\gamma < 1$, two time steps
56 in the future by γ^2 , and so on (see Materials and Methods). This is a standard assumption in
57 behavioural ecology (*Mangel and Clark, 1988; Houston and McNamara, 1999*), in which discount-
58 ing the future means that future rewards are not guaranteed but are uncertain, due to factors
59 such as interruption, consumption of a food item by a competitor, mortality, and so on. Thus
60 discounting the future represents the inherent uncertainty that animals must make decisions
61 under in their natural environments, in which their brains evolved. The appropriate discount is
62 then the probability that future rewards are realised, hence geometric discounting is optimal since
63 probabilities multiply. Indeed there is extensive evidence of such reward discounting in humans
64 and other animals (e.g. *Sellitto et al. (2010)*, although this frequently suggests hyperbolic rather
65 than geometric discounting, a fact that in itself merits an explanation based on optimality theory
66 (*McNamara and Houston, 2009*)).

67 Rederiving optimal policies to account for geometric (*Marshall, 2019*) or general multiplicative
68 (*Stevenson et al., 2019*) costs of time qualitatively changes them in the binary decision case, in-
69 troducing magnitude-sensitive reaction times (*Marshall, 2019; Stevenson et al., 2019*). However,
70 disentangling these from nonlinear subjective utility is challenging, and cannot be excluded as
71 an explanation for previous results (*Teodorescu et al., 2016; Pirrone et al., 2018a; Stevenson et al.,*
72 *2019; Zajkowski et al., 2019; Turner et al., 2019; Bhui, 2019; Smith and Krajbich, 2019; Pirrone and*
73 *Gobet, 2021*).

74 Here for the first time we extend the theoretical and experimental study of magnitude-sensitivity
75 to three-alternative decisions. We first present evidence for magnitude-sensitive reaction times in
76 three-way equal-alternative decisions. We then present optimal policy analyses and novel numerical
77 simulations for such ternary decisions, both in human subjects undertaking a psychophysical task,
78 and unicellular organisms engaged in foraging. Importantly, for a wide variety of utility functions,
79 strong magnitude-sensitivity is only observed when there is a multiplicative cost for time, rather
80 than the previously assumed linear time cost. Thus magnitude-sensitivity is revealed as genuinely
81 diagnostic for multiplicative time costing, as all other assumptions either do not generate this
82 phenomenon, or can be discounted.

83 Results

84 As we were testing theory developed to explain decision-making by animals with brains, we con-
85 ducted psychophysical experiments with human subjects. However, we also conducted foraging
86 experiments with a unicellular slime mould; testing theory across multiple species and behavioural
87 tasks increases confidence when multiple agreements with theory are observed (*Pirrone et al.,*
88 *2018a*), and slime moulds have become a model system, with multiple experiments seeking to
89 reproduce behavioural predictions from neuroscience and psychology (*Latty and Beekman, 2011;*
90 *Reid et al., 2016; Dussutour et al., 2019*).

91 Multi-Alternative Decisions in Human Psychophysical Trials are Magnitude-Sensitive
92 Here we provide strong empirical evidence for magnitude sensitivity with multiple alternatives in
93 humans, using an experimental paradigm similar to the one used to show magnitude sensitivity
94 for two-alternative decision making (*Teodorescu et al., 2016; Pirrone et al., 2018a*). Details of the
95 experiment (methods, participants, etc.) are reported in Materials and Methods. Participants had to
96 choose which of three above-threshold grey patches was brighter in an online experiment. Although
97 the experiment included conditions for which a brighter alternative existed, conditions of interest
98 were equal alternatives of different magnitude, that is, conditions for which the three patches had
99 the same brightness that could vary across magnitude conditions. Equal alternatives allow us to test
100 hypotheses regarding magnitude sensitivity, by keeping differences in evidence constant (*Pirrone*
101 *et al., 2018a,b; Pirrone and Gobet, 2021*).

102 As previously done for binary decisions (*Pirrone et al., 2018a,b*), here we focused our analyses
103 exclusively on equal alternatives. For the analyses, we did not censor any datapoints.

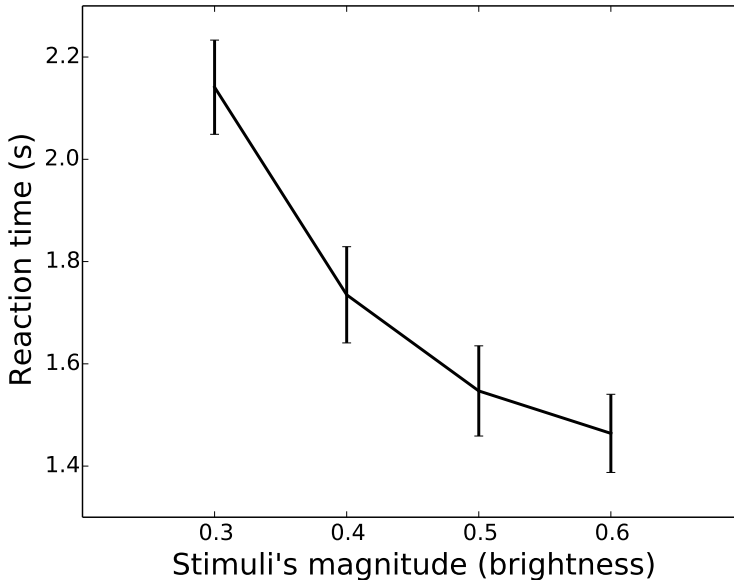


Figure 1. Empirical results from the behavioural online experiment. Decreasing reaction times as a function of the magnitude of the equal alternatives. X-axis presents mean brightness of equal alternatives (0.3, 0.4, 0.5, 0.6), on a scale of brightness from 0 to 1 in PsychoPy. Y-axis presents mean reaction times, in seconds. Bars show 95% confidence intervals. Participants experienced equal alternative conditions, interleaved with unequal alternative trials in pseudo-randomised order. Participants that performed the whole experiment experienced each equal alternative presentation ten times.

104 As shown in Figure 1, the data show strong magnitude sensitivity, given that choices for equal
105 alternatives of higher magnitude conditions (higher brightness on a scale from 0 to 1 on Python)
106 were made faster.

107 To assess if reaction times decreased as a function of the mean brightness of the equal alternatives, we used a linear mixed model in R. The model was fitted by specifying as fixed effect
108 (explanatory variable) the brightness of equal alternatives as a continuous predictor. The participant ID was also added to the model as a factor for random effects. Reaction times significantly
109 decreased as a function of the mean brightness of the alternatives ($b = -1.95$, $p < .001$, CI -2.14 -1.75).
110 Further details for the mixed-effect regression are presented in the supplementary information
111 (Table S1).

112 As the COVID-19 pandemic necessitated an online experiment we could not collect or control
113 information on a number of possible confounds (viewer position, motivation, room luminosity, etc.),
114 and there are multiple sources of unaccounted variability in our online experiment; however there
115 is no *a priori* reason to expect these to act as consistent confounds in the magnitude-sensitive
116 reaction times observed. Furthermore, the very large sample size for our study ($N = 117$; compared
117 to $N = 8$ and $N = 9$ for previous similar investigations (*Teodorescu et al., 2016; Pirrone et al.,
118 2018a*)) should minimise effects due to randomly-distributed confounds.

121 Multi-Alternative Decisions in Foraging Trials by Unicellular Organisms are Magnitude-
122 Sensitive

123 Here, using slime moulds of the species *Physarum polycephalum*, we also observed strong empirical
124 evidence for magnitude sensitivity with three alternative foraging tasks. Details of the experiment
125 are reported in Materials and Methods. Slime moulds were confronted with a choice offering three
126 equal food sources. We increased the magnitude of the options by increasing the quality of the food
127 sources. As shown in Figure 2, the latency to reach one of the alternatives depends on the quality of
128 the food sources; the higher the quality the faster the slime mould. This was confirmed by a linear
129 mixed model similar to the one applied to the human data, in which reaction times significantly
130 decreased as a function of food quality ($b = -0.03$, $p < .001$, CI -0.03 -0.02 ; further details, Table S2 in
131 the supplementary information).

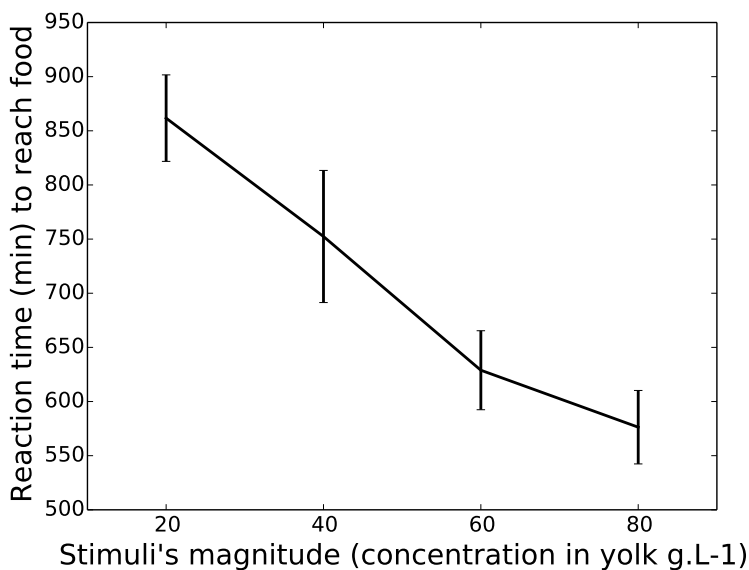


Figure 2. Empirical results from the slime mould experiment. Decreasing latencies to reach a food source as a function of the magnitude of the equal alternatives. X-axis presents the concentration in egg yolk of equal food sources (20, 40, 60, 80 g.L-1). Y-axis presents mean latency to reach a food source, in minutes. Bars show 95% confidence intervals. 50 slime moulds were tested for each magnitude for a total of 200 slime moulds.

132 **Optimal Policies**

133 For our theoretical analysis we begin by re-deriving optimal policies for decisions when the change
134 is made from linear costing of time, or Bayes Risk, to geometric discounting of future reward. Note
135 that geometric discounting of future rewards is similar to, but not the same as, non-linear utility. As
136 remarked in the introduction above, for binary decisions magnitude-sensitive reaction times can be
137 explained by optimal decision policies for either multiplicative (e.g. geometric) time discounting
138 (*Marshall, 2019; Stevenson et al., 2019*) or nonlinear subjective utility with linear time costs (*Tajima*
139 *et al., 2016*). In the multi-alternative case, on the other hand, the picture is more nuanced; moving
140 from linear costing of time to geometric discounting of future rewards changes complicated time-

141 dependent non-linear decision thresholds ((*Tajima et al., 2019*) Fig. 7) into either simple linear ones
 142 that collapse over time for lower-value option sets (Fig. 3), or nonlinear boundaries that evolve
 143 over time similarly to the Bayes Risk-optimising case for higher-value option sets (*Marshall (2019)*;
 144 Fig. 3). As *Tajima et al.* note, the simpler linear decision boundaries implement the 'best-vs-average'
 145 decision strategy, whereas the more complex boundaries interpolate between 'best-vs-average'
 146 and 'best-vs-next' decision strategies (*Tajima et al., 2019*); interestingly simply moving to nonlinear
 147 subjective utility with linear time costs simplifies the decision strategy to the 'best-vs-next' strategy
 148 (Fig. 3; see *Tajima et al. (2019)*, Fig. 6C).

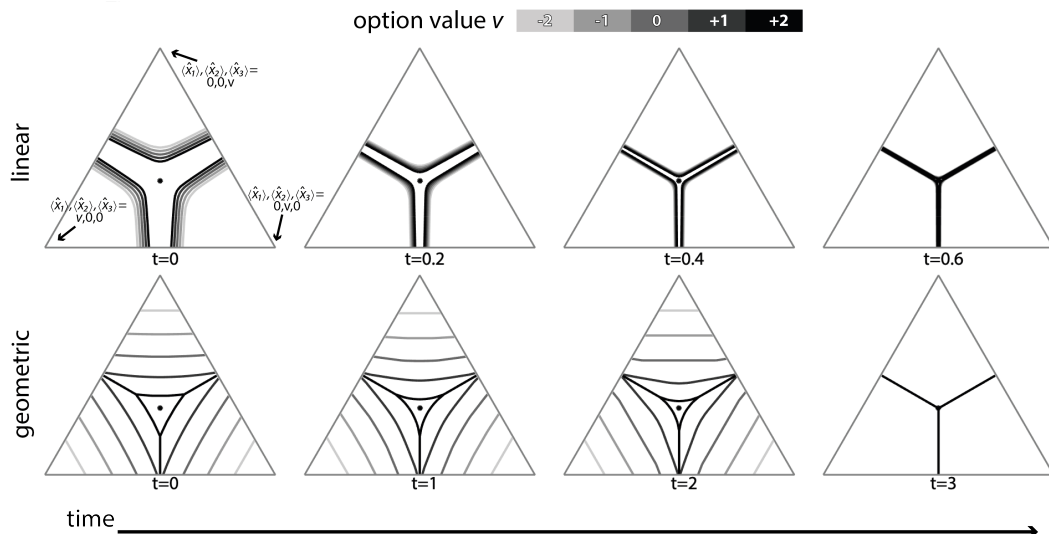


Figure 3. Linear time costs lead to weakly magnitude-sensitive optimal policies (top row), while geometric discounting of reward leads to strongly magnitude-sensitive optimal policies (bottom row). In the linear time cost (Bayes Risk) case nonlinear subjective utility changes complex time and value-dependent decision boundaries in estimate space into a simple mostly magnitude-insensitive 'best-vs-next' strategy (top row; see *Tajima et al. (2019)*, Fig. 6C). For geometric discounting of rewards over time, optimal decision boundaries are strongly magnitude-sensitive and interpolate between simple 'best-vs-average' and 'best-vs-next' strategies (see *Tajima et al. (2019)*, Fig. 6). Triangles are low dimensional projections of the 3-dimensional evidence estimate space onto a plane moving along the equal value line, at value v (*Tajima et al., 2019*). Dynamic programming parameters were: prior mean $\bar{x}_{p,i} = 1.5$ and variance $\sigma_{p,i}^2 = 5$, waiting time $t_w = 1$, temporal costs $c = 0$, $\gamma = 0.2$, and utility function parameters $m = 4$, $s = 0.25$ (for the linear time cost) and $m = 4$, $s = 3.5$ (for the geometric time cost).

149 Multi-Alternative Decisions: Optimal Policies are Weakly Magnitude-Sensitive for Nonlin-
 150 ear Subjective Utility Under Bayes Risk-Optimisation

151 Under Bayes Risk-optimisation it is known that, for binary decisions, optimal policies are magnitude-
 152 insensitive when subjective utility is linear, whereas they are magnitude-sensitive when subjective
 153 utility is nonlinear (*Tajima et al., 2016, 2019*).

154 For ternary decisions, however, even with nonlinear subjective utility, policies exhibit very weak
 155 magnitude-sensitivity early in decisions, becoming magnitude-insensitive as decisions progress
 156 (Fig. 3, row 'linear'). Sensitivity analysis shows that magnitude-insensitivity is a general pattern. An
 157 informal understanding of this can be arrived at by appreciating that sigmoidal functions have

158 two extremes of parameterisation; in one extreme they are almost linear, hence will be mostly
 159 magnitude insensitive due to the known result (*Tajima et al., 2016*). At the other extreme, the
 160 function becomes step-like; in this case options are either good or bad, and the optimal policy
 161 rapidly becomes 'choose the best' (Fig. 4), since under such a scenario sampling is of minimal benefit
 162 as early information quickly indicates whether an option is good or bad, and choosing the first
 163 option that appears to be good is optimal.

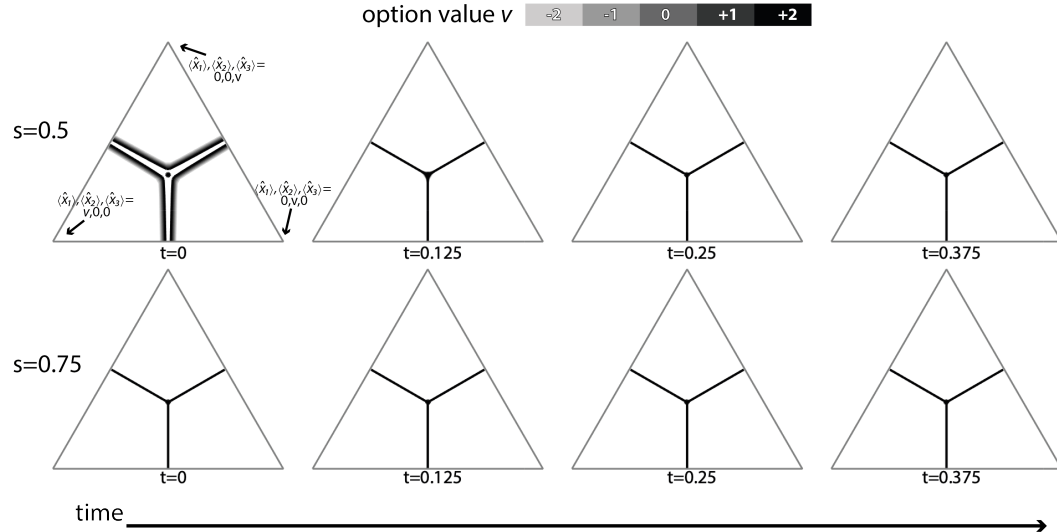


Figure 4. Optimal policies for linear time cost (Bayes Risk) rapidly transition from approximately linear subjective utility, and hence weakly magnitude-sensitive, decision boundaries in estimate space (Fig. 3, top row for $s = 0.25$; present figure, top row for $s = 0.5$, to more step-like subjective utility where immediate 'choose the best' decision-boundaries are necessarily magnitude-insensitive (bottom row for $s = 0.75$, and higher values of s). Triangles are low dimensional projections of the 3-dimensional evidence estimate space onto a plane moving along the equal value line, at value v (*Tajima et al., 2019*). Dynamic programming parameters were: prior mean $\bar{x}_{p,i} = 1.5$ and variance $\sigma_{p,i}^2 = 5$, and utility function parameters $m = 4$, $s \in \{0.5, 0.75\}$.

164 Multi-Alternative Decisions: Optimal Policies Become Magnitude-Sensitive Under Geo-
 165 metric Discounting
 166 As previously shown (*Marshall, 2019; Stevenson et al., 2019*), assuming geometric temporal dis-
 167 counting, the optimal policy for binary decisions is magnitude-sensitive. In ternary decisions,
 168 geometric discounting has the same effect; regardless of utility function linearity, the optimal policy
 169 is magnitude-sensitive (Fig. 3, row 'geometric').

170 Numerical Simulations

171 Since noise-processing is fundamental in determining reaction times, we confirmed the results on
 172 magnitude sensitivity from our optimal policy analysis via numerical simulation of Bayes-optimal
 173 evidence-accumulating agents using those policies (see Materials and Methods). These numerical
 174 simulations confirmed the qualitative results from the optimal policy analysis; reaction times for
 175 ternary decisions under linear time costing are only weakly magnitude sensitive even for nonlinear

176 subjective utility functions, while under geometric time costing reaction times become strongly
177 magnitude sensitive for most utility functions examined.

178 **Multi-Alternative Decisions: Simulated Reaction Times are Weakly Magnitude-Sensitive
179 for Nonlinear Subjective Utility Under Bayes Risk-Optimisation**

180 Across all nonlinear subjective utility functions considered, linear time costing resulted in weakly
181 magnitude-sensitive simulated reaction times (Fig. 5). This agrees with the weak magnitude-
182 sensitivity observed in the optimal policies derived above (Fig. 3). Note, however, that this contrasts
183 with the binary decision case in which optimal policies, and hence reaction times, become magnitude
184 sensitive under linear time cost when subjective utility is nonlinear (*Tajima et al., 2016*). An informal
185 justification for this is given above in analysis the optimal decision boundaries computed via
186 dynamic programming.

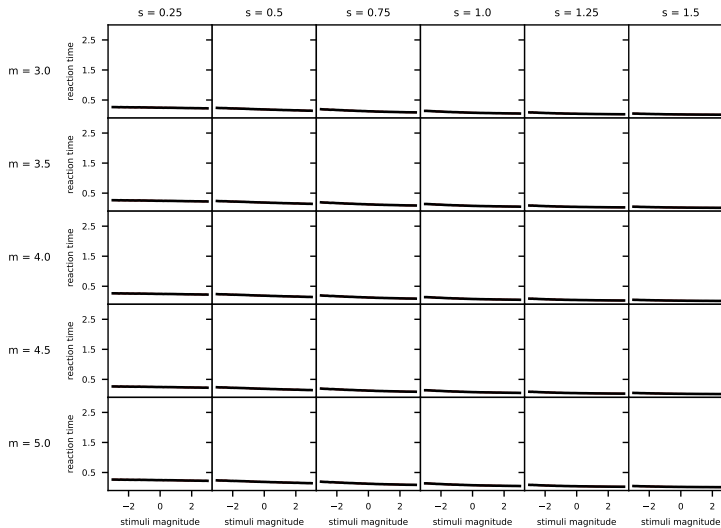


Figure 5. Linear time costs lead to weakly magnitude-sensitive simulated reaction times across a range of nonlinear subjective utility functions for equal value option sets. Simulation parameters were: prior mean $\bar{x}_{p,i} = 1.5$ and variance $\sigma_{p,i}^2 = 5$, observation noise variance $\sigma_{a,i}^2 = 2$, temporal cost $c = 0$, waiting time $t_w = 1$, and simulation timestep $dt = 5 \times 10^{-3}$. Lines are the mean reaction time for 10^4 simulations, 95% confidence intervals are shown as red shading (mostly invisible because smaller than the linewidth).

187 **Multi-Alternative Decisions: Simulated Reaction Times Become Magnitude-Sensitive Under
188 Geometric Discounting**

189 In contrast to linear time costing, across all nonlinear subjective utility functions considered, geo-
190 metric time costing resulted in strongly magnitude sensitive simulated reaction times (Fig. 6),
191 with longer reaction times for lower value equal-value option sets; this strategy was previously
192 hypothesised to be optimal (*Pais et al., 2013*). The strong magnitude-sensitivity in the numerical
193 simulations corresponds with the strong magnitude-sensitivity observed in the optimal policies
194 derived above (Fig. 3).

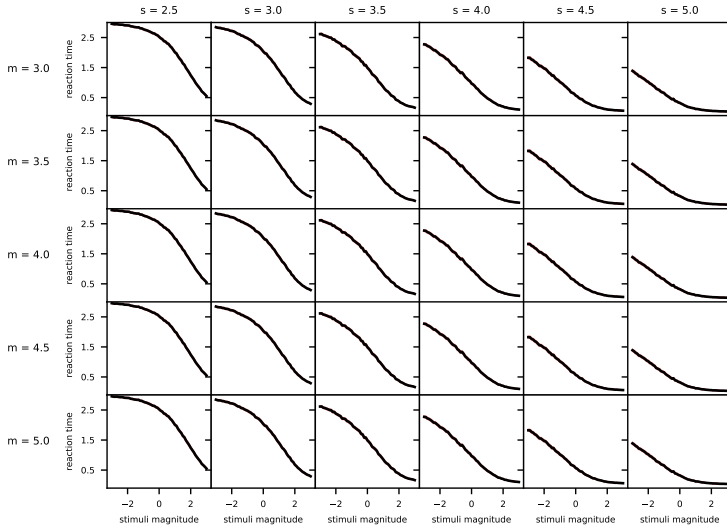


Figure 6. Geometric discounting of reward leads to strongly magnitude-sensitive simulated reaction times across a range of nonlinear subjective utility functions, with decisions postponed for low equal-value option sets. Simulation parameters were: prior mean $\bar{x}_{p,i} = 1.5$ and variance $\sigma_{p,i}^2 = 5$, observation noise variance $\sigma_{a,i}^2 = 2$, temporal cost $\gamma = 0.1$, and simulation timestep $dt = 5 \times 10^{-3}$. Lines are the mean reaction time for 10^4 simulations, 95% confidence intervals are shown as red shading (mostly invisible because smaller than the linewidth).

195 Discussion

196 In understanding behaviour, which is a product of evolution, searching for optimal algorithms for
197 typical decision problems can provide great insight. This normative approach can explain observed
198 behaviours, and predict new behavioural patterns, based on evolutionary advantage. Yet the
199 assumptions underlying such model analyses can prove crucial. Recently it has been asked what
200 optimal decision algorithms look like for multi-alternative value-based choices, in which subjects are
201 rewarded not by whether their decision was correct or not, but by the value to them of the selected
202 option (*Tajima et al., 2019*). The resulting algorithms correspond to earlier simple models for
203 perceptual and value-based decision-making. These findings, however, rest on an assumption that
204 time is a linear cost for subjects. Here we have shown that deciding human subjects and foraging
205 unicellular organisms do, however, exhibit marked magnitude sensitivity in ternary decisions, as
206 previously shown for binary decisions (*Pirrone et al., 2018a; Dussutour et al., 2019*). We have also
207 shown that optimality theory that discounts future rewards multiplicatively based on time is the
208 foremost explanation for such observations of magnitude-sensitivity; nonlinear subjective utility
209 alone is not sufficient to give rise to strongly magnitude-sensitive decision times when time is
210 treated as a linear cost.

211 Behavioural Predictions

212 The Bayes Risk optimal policy is approximated by a neural model that is consistent with observations
213 of economic irrationality (*Tajima et al., 2019*), hence it will be important to see if a revised neural

214 model based on the revised optimal policy still shows such agreement. For example, while in the
215 binary case magnitude-sensitive reaction times can be explained both by nonlinear subjective utility
216 functions, and by multiplicative discounting rather than Bayes Risk, in the multi-alternative case our
217 analysis suggests that the same phenomenon is explained *primarily* by multiplicative discounting of
218 future rewards and not by nonlinear utility.

219 **Optimality Criteria**

220 Practitioners of behavioural ecology have established principles to deal with empirically-observed
221 deviations from the predictions of optimality theory (*Parker and Smith, 1990*); two of the most
222 useful are to consider that the optimisation criterion has been misidentified, or the behaviour in
223 question is not really adaptive. Tajima and colleagues employ an exemplary approach, attempting
224 to combine the best of the approaches of normative and mechanistic modelling (*McNamara and*
225 *Houston, 2009*); yet it bears remembering that subjects may not be trying optimally to solve the
226 simple decision problem they are presented in the lab, but rather making use of mechanisms that
227 evolved to solve the problem of living in their natural environment (*Fawcett et al., 2014*); indeed
228 the experimental data presented here were produced by subjects who received no reward, yet
229 nevertheless acted as if they were making an economic, value-based, decision rather than a purely
230 perceptual, accuracy-based one.

231 **Materials and Methods**

232 **Psychophysical Experiment**

233 **Participants**

234 This experiment was conducted during the COVID-19 pandemic, from May 13th – June 1st 2020..
235 Given that it was not possible to recruit participants for a laboratory experiment, we instead
236 recruited them online using Pavlovia (*Peirce et al., 2019; Peirce, 2007*), an online platform for
237 psychophysical experiments implemented in PsychoPy.

238 Running a perceptual experiment online has a number of limitations: first, there is no way to
239 ensure that participants are focused on the task and minimising distractions - to mitigate this we
240 kept the task short and participants were instructed to concentrate on it; second, Pavlovia (as of
241 March-May 2020) only allows stimuli to be drawn in units relative to window size (i.e., the window in
242 which the experiment is displayed) or in pixels, hence their size and position relative to the fixation
243 cross will vary across devices, depending on specific window sizes. However, even if the size and
244 location of stimuli could be kept constant across participants, participants' distance from the screen
245 cannot be controlled during an online experiment.

246 While in previous two-alternative experiments (*Teodorescu et al., 2016; Pirrone et al., 2018a*)
247 a limited number of participants ($N < 10$) performed a large number of trials, for our online
248 experiment we aimed at a large number of participants performing a limited number of trials.

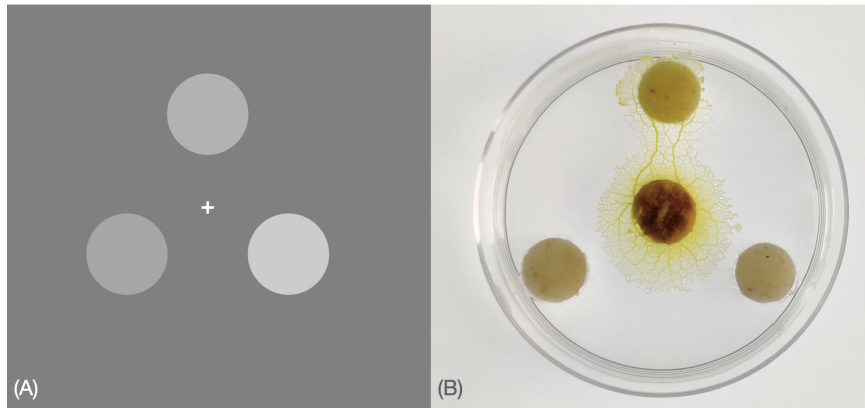


Figure 7. (A) Stimuli example for human psychophysical experiments: Participants were requested to decide as fast and accurately as possible which of the three stimuli was brighter; they were asked to maintain fixation on the cross at the centre of the screen and minimise distraction for the short duration of the experiment. Unknown to participants, conditions of interest were conditions for which the stimuli had equal mean brightness. (B) Photograph showing a slime mould that chose one food alternative among three equal ones. The slime mould was placed in the centre of a petri dish (6cm Ø) filled with agar gel (10 g/l) at a distance of 2cm from each food alternative.

249 This strategy is beneficial for online studies since the large number of participants helps ensure
250 that variation in participants' motivation or viewing arrangements is averaged out. We therefore
251 recruited 117 participants via external advertisement on Twitter, and internal email lists at the
252 University of Sheffield (mean age = 40.4, SD = 11.2774, range 23 -77; 79 females, 37 males, 1 did
253 not indicate their gender). We requested participants to follow the link to the experiment only if
254 aged 18 years or older. The experiment lasted about 5 minutes and participation was voluntary;
255 participants did not receive any reward for their participation.

256 After reading the instructions, participants were informed that by continuing they were confirming
257 that they understood the nature of the experiment and consented to participate. Participants
258 were also informed that they could leave the experiment at any time by closing the browser. For this
259 experiment, all procedures were approved by the University of Sheffield, Department of Computer
260 Science Ethics Committee.

261 **Experimental setup**

262 Similarly to previous studies (*Teodorescu et al., 2016; Pirrone et al., 2018a*), stimuli consisted of
263 three homogeneous, round, white patches in a triangular arrangement on a grey background, as
264 depicted in Figure 7. Throughout the task participants were presented with a central fixation cross
265 that they were requested to fixate on.

266 On a scale from 0 to 1 in PsychoPy, the patches could have a brightness of 0.3, 0.4, 0.5 or 0.6.
267 There were $4^3 = 64$ possible trial combinations, of which 4 were equal alternatives (i.e., alternatives
268 having a brightness of [0.3,0.3,0.3], [0.4,0.4,0.4], [0.5,0.5,0.5] or [0.6,0.6,0.6]). We selected 10 equal
269 trial repeats, and only one trial repeat for all possible unequal alternatives, for a total of 100

270 trials per participant. On each frame, a Gaussian random variable with mean 0 and standard
271 deviation of $0.25 \times$ (mean brightness of the alternative) was added separately to the brightness
272 level of each patch; the signal-to-noise ratio was thus kept constant across equal alternatives of
273 different magnitude. The order of presentation of the alternatives was pseudo-randomised across
274 participants and there was no systematic link between patch position and best option.

275 Three grey patches were presented simultaneously on the screen and subjects were asked to
276 decide which of the three was brighter by pressing 'left', 'right' or 'up' on a keyboard using their
277 second, fourth or third right-hand fingers, via a line-drawn diagram of a hand over a keyboard
278 presented before the experiment began; specific instructions for left-handed participants were not
279 provided, and we did not record handedness. The inter-trial interval, during which participants
280 were presented with only the fixation cross, was selected at random between 0.5 seconds, 1 second
281 or 1.5 seconds for each trial. Subjects were instructed to be as fast and accurate as possible and to
282 maintain their fixation on the cross at the centre of the screen throughout the experiment. Before
283 the experiment they were presented with 6 training trials (unequal alternatives) to familiarise
284 themselves with the task. Participants were not provided with any feedback after each trial and
285 were not informed about the presence of the equal-alternatives conditions.

286 Slime Mould Experiment

287 *Physarum polycephalum*, also known as the acellular slime mould, is a giant polynucleated single cell
288 organism that inhabits shady, cool, and moist areas. In the wild, *P. polycephalum* eats bacteria and
289 dead organic matter. In the presence of chemical stimuli in the environment, slime moulds show
290 directional movements (*i.e.* chemotaxis).

291 Slime moulds of strain LU352 kindly provided by Professor Dr Wolfgang Marwan (Max Planck
292 Institute for Dynamics of Complex Technical Systems, Magdeburg, Germany) were used for the
293 experiments. Slime moulds were initiated with a total of 10 sclerotia which are encysted resting
294 stages. The sclerotia were soaked in water and placed in petri dishes (140 mm \varnothing) on agar gel
295 (1%). Once revived, slime moulds start to explore the agar gel, usually 24h after the reactivation of
296 the sclerotia. The slime moulds were then reared for a month on a 1% agar medium with rolled
297 oat flakes (Quaker Oats Company®) in Petri dishes (140 mm \varnothing). They were kept in the dark in a
298 thermoregulated chamber at a temperature of 20 degrees Celsius and a humidity of 80%. The day
299 before the experiment the slime moulds were transferred on a 10% oat medium (powdered oat
300 in a 1% agar solution) in Petri dishes (diameter 140 mm). The experiments were carried out in a
301 thermoregulated chamber and pictures were taken with a Canon 70D digital camera.

302 Slime moulds were presented with a choice between three equal food sources in an arena
303 consisting of 60 mm diameter Petri dish filled with plain 1% agar. We punched three holes (10mm
304 \varnothing) in the arena and filled them with a food source (10mm \varnothing). We used four different food patches
305 varying in quality: 2% w/v powdered oat mixed with either 2, 4, 6 or 8% w/v egg yolk. Once the

306 food sources were set in each hole, we placed a slime mould (10mm \varnothing) in the centre of the arena
307 2cm away from each food. We replicated the experiment 50 times for each food quality. For each
308 replicate, we measured the time taken by the slime mould to reach either one of the three food
309 sources.

310 To assess the difference in the latency to reach the food as a function of the food quality, we
311 used a linear mixed model (function lmer, Package lme4) in R (RStudio Version 1.2.1335). The
312 models were fitted by specifying the fixed effects (explanatory variables) the concentration in yolk
313 (continuous predictor). The sclerota identity was also added to the model as a random factor. We
314 transformed the dependant variable using the "bestNormalize" function ("bestNormalize" package).
315 The outcome of the model is presented in the supplementary information (Table S2).

316 **Optimal policies**

317 Optimal policy computations were performed in Matlab (*MathWorks, 2020*), and were adapted
318 from the dynamic program of *Tajima et al. (2019)*. Optimal policies were computed for Bayes Risk
319 and geometric discounting, for linear utility ($r := x$), and for non-linear utility functions having the
320 form

$$r := m \left(\frac{1}{1 + e^{-sx}} - 1 \right) \quad (1)$$

321 where m and s are shape parameters for the logistic function determining the interval of utilities
322 and steepness of the slope respectively, and x is the raw input value. We systematically varied the
323 m and s parameters to test magnitude-sensitivity under Bayes Risk optimisation and geometric
324 discounting, under a range of utility function shapes ranging from almost linear, to almost stepwise.
325 Note that a sigmoid curve includes an interval in which subjective utility is an accelerating function
326 of input value when the latter is negative, and an interval in which it is a decelerating function when
327 the latter is positive; thus testing for magnitude-sensitivity over the full interval of raw input values
328 tests a variety of utility function shapes over sub-intervals.

329 The Bellman equation used in the dynamic programming analysis for the Bayes Risk-optimisation
330 case was

$$V(t, \hat{x}(t)) = \max \{ \max_i \{ r_i(t, \hat{x}(t)) \} - \rho t_w, \langle V(t + \delta t, \hat{x}(t + \delta t)) \rangle - (c + \rho) \delta t \}, \quad (2)$$

331 where $V(t, \hat{x}(t))$ is the value of the state estimates vector $\hat{x}(t)$ at time t , $r_i(t, \hat{x}(t))$ is similarly the
332 expected reward from choosing the i -th reward, δt is the time interval to the next decision point, c
333 is the linear cost per unit time, ρ is the reward rate per unit time based on optimal decision-making
334 over a sequence of trials, t_w is the inter-trial waiting time, and $\langle \dots \rangle$ is expectation over the next time
335 interval (δt) (*Tajima et al., 2019*). For the results presented here we set $c = 0$, $t_w = 1$ and found the
336 optimal $\rho > 0$ using the methods of *Tajima et al. (2019)*; note, however, that since the prior was not
337 varied this reward-rate optimisation could not induce magnitude-sensitive reaction times in itself.

338 For the geometric discounting case the Bellman equation becomes

$$V(t, \hat{\mathbf{x}}(t)) = \max \{ \max_i \{ r_i(t, \hat{\mathbf{x}}(t)) \}, \langle V(t + \delta t, \hat{\mathbf{x}}(t + \delta t)) \rangle^\gamma \}, \quad (3)$$

339 where $0 < \gamma < 1$ is a discount factor for rewards received in future timesteps; this discount factor is
340 per-unit-time, hence to discount a reward $\delta t < 1$ timesteps in the future the appropriate factor is
341 $\gamma^{\delta t/1} = \gamma^{\delta t}$.

342 **Stochastic simulations**

343 Since noise processing is important in determining reaction times, we derived optimal decision
344 policies as above, then tested them through numerical analysis of stochastic models. To test for
345 magnitude-sensitive decision-making we examined the case of $n = 3$ equal-quality alternatives, in
346 which we varied the magnitude of the (equal) stimuli values. Through these stochastic simulations,
347 we tested the impact of the different temporal discount methods—linear or geometric—and of
348 different utility functions—linear or nonlinear—on the decision speed (reaction time RT). The
349 stochastic models simulate the sequential accumulation of evidence for the three alternatives
350 $i \in \{1, 2, 3\}$ that are used to compute the expected rewards $\langle \hat{x}_i(t) \rangle$. The three evidence estimates
351 can be represented, with a little abuse of notation, as a vector $\hat{\mathbf{x}}(t)$ denoting a point in a cube that
352 represents the estimate space. In that cube, we also include the decision boundaries computed
353 as above, indicating the separation of the estimate space into decision regions; in one region
354 continuing to sample is expected to maximise utility, and in the other region taking a decision for
355 the leading option is expected to be the best action.

356 In our simulations, each time step of length dt the decision-maker accumulates three pieces of
357 evidence, one for each option. Evidence for an option i is sampled from the normal distribution
358 $\mathbf{X}_i \sim \mathcal{N}(\bar{x}_i dt, \sigma_{a,i}^2 dt)$, where each sample $x_{\tau,i}$ is a piece of momentary evidence at a small timestep
359 of length dt and with sequential index τ , \bar{x}_i is the true raw value (before any nonlinear utility
360 transformation) of option i and $\sigma_{a,i}^2$ is the variance in accumulation of evidence for i (Tajima et al.,
361 2016). Before observing any evidence, the decision maker has prior mean and variance, $\bar{x}_{p,i}$ and
362 $\sigma_{p,i}^2$ for the distribution of \mathbf{X}_i . Each new piece of accumulated evidence is used by the decision
363 maker to update the posterior expected reward as

$$\langle \hat{x}_i(t) \rangle = \frac{\bar{x}_{p,i} \sigma_{a,i}^2 + \sum_{\tau=1}^t dx_{\tau,i}}{\sigma_{a,i}^2 + \sigma_{p,i}^2 t}. \quad (4)$$

364 **Code and Data Availability**

365 Optimisation codes for the results presented here can be downloaded from

366 <https://github.com/DiODEProject/MultiAlternativeDecisions/tree/stochastic-sim>

367 Experimental code and data for the results presented here can be downloaded from

368 <https://osf.io/8jumk/>

369 Acknowledgements

370 We thank Satohiro Tajima for sharing the code for the binary decision model. Dr Tajima was an
371 exceptionally promising scientist who is sadly missed. We thank Jan Drugowitsch and Alex Pouget
372 for discussions of their results and our own, and Thomas Bose, Nathan Lepora and Sophie Baker
373 for comments on an earlier draft.

374 Declaration of Conflicting Interests

375 The authors declare that they have no conflicting interests.

376 References

377 Bhui, R. (2019). Testing optimal timing in value-linked decision making. *Computational Brain & Behavior*, 2(2):85–
378 94.

379 Bogacz, R., Brown, E., Moehlis, J., Holmes, P., and Cohen, J. D. (2006). The physics of optimal decision making:
380 a formal analysis of models of performance in two-alternative forced-choice tasks. *Psychological Review*,
381 113(4):700.

382 Dussutour, A., Ma, Q., and Sumpter, D. (2019). Phenotypic variability predicts decision accuracy in unicellular
383 organisms. *Proceedings of the Royal Society B*, 286(1896):20182825.

384 Fawcett, T. W., Fallenstein, B., Higginson, A. D., Houston, A. I., Mallpress, D. E., Trimmer, P. C., and McNamara, J. M.
385 (2014). The evolution of decision rules in complex environments. *Trends in Cognitive Sciences*, 18(3):153–161.

386 Fudenberg, D., Strack, P., and Strzalecki, T. (2018). Speed, accuracy, and the optimal timing of choices. *American
387 Economic Review*, 108(12):3651–84.

388 Houston, A. I. and McNamara, J. M. (1999). *Models of adaptive behaviour: an approach based on state*. Cambridge
389 University Press.

390 Krajbich, I., Armel, C., and Rangel, A. (2010). Visual fixations and the computation and comparison of value in
391 simple choice. *Nature neuroscience*, 13(10):1292–1298.

392 Latty, T. and Beekman, M. (2011). Speed–accuracy trade-offs during foraging decisions in the acellular slime
393 mould *physarum polycephalum*. *Proceedings of the Royal Society B: Biological Sciences*, 278(1705):539–545.

394 Mangel, M. and Clark, C. W. (1988). *Dynamic modeling in behavioral ecology*. Princeton University Press.

395 Marshall, J. A. R. (2019). Comment on ‘optimal policy for multi-alternative decisions’. *bioRxiv*.

396 MathWorks (2020). Matlab r2020b.

397 McNamara, J. M. and Houston, A. I. (2009). Integrating function and mechanism. *Trends in Ecology & Evolution*,
398 24(12):670–675.

399 Pais, D., Hogan, P. M., Schlegel, T., Franks, N. R., Leonard, N. E., and Marshall, J. A. R. (2013). A mechanism for
400 value-sensitive decision-making. *PloS one*, 8(9):e73216.

401 Parker, G. A. and Smith, J. M. (1990). Optimality theory in evolutionary biology. *Nature*, 348(6296):27.

402 Peirce, J., Gray, J. R., Simpson, S., MacAskill, M., Höchenberger, R., Sogo, H., Kastman, E., and Lindeløv, J. K. (2019).
403 Psychopy2: Experiments in behavior made easy. *Behavior research methods*, 51(1):195–203.

404 Peirce, J. W. (2007). Psychopy—psychophysics software in python. *Journal of neuroscience methods*, 162(1-2):8–13.

405 Pirrone, A., Azab, H., Hayden, B. Y., Stafford, T., and Marshall, J. A. (2018a). Evidence for the speed-value trade-off:
406 Human and monkey decision making is magnitude sensitive. *Decision*, 5(2):129.

407 Pirrone, A. and Gobet, F. (2021). Is attentional discounting in value-based decision making magnitude sensitive?
408 *Journal of Cognitive Psychology*.

409 Pirrone, A., Stafford, T., and Marshall, J. A. R. (2014). When natural selection should optimize speed-accuracy
410 trade-offs. *Frontiers in neuroscience*, 8:73.

411 Pirrone, A., Wen, W., and Li, S. (2018b). Single-trial dynamics explain magnitude sensitive decision making. *BMC
412 neuroscience*, 19(1):1–10.

413 Reid, C. R., MacDonald, H., Mann, R. P., Marshall, J. A., Latty, T., and Garnier, S. (2016). Decision-making without
414 a brain: how an amoeboid organism solves the two-armed bandit. *Journal of The Royal Society Interface*,
415 13(119):20160030.

416 Sellitto, M., Ciaramelli, E., and di Pellegrino, G. (2010). Myopic discounting of future rewards after medial
417 orbitofrontal damage in humans. *Journal of Neuroscience*, 30(49):16429–16436.

418 Smith, S. M. and Krajbich, I. (2019). Gaze amplifies value in decision making. *Psychological Science*, 30(1):116–128.

419 Steverson, K., Chung, H.-K., Zimmermann, J., Louie, K., and Glimcher, P. (2019). Sensitivity of reaction time to the
420 magnitude of rewards reveals the cost-structure of time. *Scientific Reports*, 9(1):1–14.

421 Tajima, S., Drugowitsch, J., Patel, N., and Pouget, A. (2019). Optimal policy for multi-alternative decisions. *Nature
422 Neuroscience*, 22:1503–1511.

423 Tajima, S., Drugowitsch, J., and Pouget, A. (2016). Optimal policy for value-based decision-making. *Nature
424 Communications*, 7:12400.

425 Teodorescu, A. R., Moran, R., and Usher, M. (2016). Absolutely relative or relatively absolute: violations of value
426 invariance in human decision making. *Psychonomic Bulletin & Review*, 23(1):22–38.

427 Turner, W., Feuerriegel, D., Andrejevic, M., Hester, R., and Bode, S. (2019). Perceptual change-of-mind decisions
428 are sensitive to absolute evidence magnitude. *PsyArXiv*.

429 Zajkowski, W., Krzemiński, D., Barone, J., Evans, L., and Zhang, J. (2019). Reward certainty and preference bias
430 selectively shape voluntary decisions. *bioRxiv*, page 832311.